

Sub-Coulomb Transfer in Collisions of  $^{238}\text{U}$  with  $^{238}\text{U}^B$

G. Wirth, W. Brüchele, M. Brügger, H. Gäggeler, K. Sümmerer  
 GSI Darmstadt  
 J. V. Kratz, M. Lerch, N. Trautmann  
 Institut für Kernchemie, Universität Mainz

Only little is known about the reaction of quasi-elastic transfer reactions as well as about the onset of damped collisions between very heavy ions at incident energies near and below the Coulomb-barrier[1]. This information would be of special interest for the interaction of  $^{238}\text{U}$  with  $^{238}\text{U}$ . In that case positron lines were observed at beam energies 5.7 MeV/u - 6.1 MeV/u and the existence of a long-lived ( $\sim 10^{-20}$  s) giant nuclear U-U-complex was suggested[2] If long-lived giant nuclear complexes exist, this could possibly show up in the cross sections and angular distributions of transfer products.

In a previous report[3], it has been shown that the integral cross sections for the formation of the surviving transfer product  $^{239}\text{U}$  in the reaction  $^{238}\text{U} + ^{238}\text{U}$  over a wide energy range from the Coulomb barrier down to 73% of the barrier behaves as expected from semiclassical considerations. In addition angular distributions for  $^{239}\text{U}$  have been measured at angles from  $180^\circ$  to  $45^\circ$  in the laboratory and at various energies. The angular range was chosen to avoid contaminations from transfer products of the beam with light target impurities like oxygen or with the carbon target-backing. Fig. 1 shows the transfer probability versus the overlap-parameter  $d_o = R_{\text{MIN}}/(A_1^{1/3} + A_2^{1/3})$ , where  $R_{\text{MIN}}$  is determined by the scattering angle assuming pure Rutherford trajectories. Corrections of 50%, 25% and 12% for target-like contributions have been applied at all energies for the three data points nearest to the  $45^\circ_{\text{lab}}$  angle ( $45^\circ_{\text{lab}}$  corresponds to the highest  $d_o$  value of each energy) respectively. According to the semiclassical description the transfer probability should scale with the distance of closest approach and all data points in Fig. 1 are expected to fall on a straight line. The strong deviation of the experimental values from that straight line at  $d_o \leq 1.45$  is very likely due to absorption out of the quasi-elastic channel. But still in collisions with much less nuclear overlap (i.e. higher  $d_o$ -values) deviations are observed. As one can see from Fig. 1 at all energies always for the central colli-

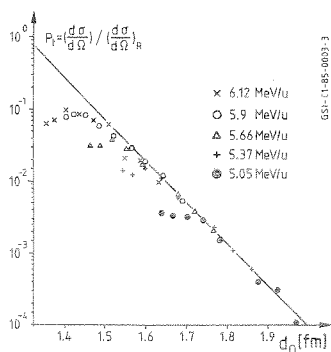


Fig.1: Transfer probability calculated from the differential cross section of the 1n-transfer product  $^{239}\text{U}$  and the Rutherford cross section as a function of  $d_o = R_{\text{MIN}}/(A_1^{1/3} + A_2^{1/3})$  in the reaction  $^{238}\text{U} + ^{238}\text{U}$ .

sions the transfer probability is less than expected. At the moment it is an open question, whether this is an experimental problem or a real physical effect. One has to keep in mind, that for a symmetric system in central quasi-elastic collisions the projectile-like transfer products have very low velocities in the laboratory. Straggling effects in the target might then modify the angular distributions for the largest laboratory angles.

Fig. 2 shows cross sections for the formation of more complex transfer products. If no cross section is given for a certain isotope in Fig. 2 this means that due to unfavourable decay characteristics this isotope could not be detected with a sensitivity comparable to cross sections of observed neighbouring nuclei. But what clearly can be seen is that even at energies below the nominal barrier the transfer of many nucleons is observed as for example a 2p9n-transfer with  $8 \mu\text{b}$  at 5.9 MeV/u ( $0.95 \cdot B$ ). The reaction mechanism leading to the more complex transfer channels seems to be different from the quasi-elastic 1n- and 2n-transfers. To get a better understanding of their origin it is planned to measure angular distributions for the more complex transfer channels as well as cross sections for the fission component. In order to look for a signature of a long-lived giant nuclear complex we will try to find complex transfer products at lower beam energies, where even for central collisions the nuclear overlap should not be sufficient to allow for many-nucleon transfer in 'trivial' damped collisions. This should be indicated by a strong decrease of the fission component.

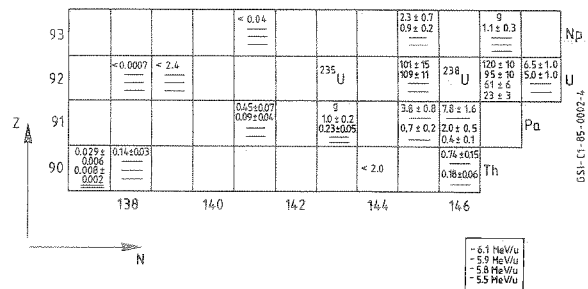


Fig.2: Cross sections in mb for the formation of various surviving transfer products at different energies in the reaction  $^{238}\text{U} + ^{238}\text{U}$ .

References

1. H. Siekmann et al., Z. Physik A307, 113 (1982)
2. P. Kienle, GSI-84-60, Preprint October 1984  
 B. Müller, GSI-84-62, Preprint October 1984
3. G. Wirth et al., GSI 83-1, 13 (1983)

Mass and charge distributions in  $^{50}\text{Ti}$ ,  $^{54}\text{Cr}$  and  $^{58}\text{Fe}$  - induced<sup>B</sup>

reactions with  $^{207,208}\text{Pb}$  and  $^{209}\text{Bi}$

H. Keller, R. Bellwied, K. Lützenkirchen, J.V. Kratz  
 Institut für Kernchemie der Universität Mainz

W. Brühle, K.J. Moody, M. Schädel  
 GSI Darmstadt

During experiments at the velocity filter SHIP in which isotopes of elements 104, 106, 108 and 109 were produced in fusion reactions between  $^{50}\text{Ti}$ ,  $^{54}\text{Cr}$ , and  $^{58}\text{Fe}$  projectiles and  $^{207,208}\text{Pb}$  and  $^{209}\text{Bi}$  targets, we installed catcher foils close to the target in order to collect parasitically products from deep inelastic transfer and fragments from fusion-like processes.

Complete mass and charge distributions were determined for the  $^{50}\text{Ti}$  bombardment at 4.85 MeV/A, for the  $^{54}\text{Cr}$  bombardment at 4.90 MeV and for  $^{58}\text{Fe}$  at 5.02 MeV, by separating the collected activities into  $\leq 20$  chemical fractions which were then subject to  $\alpha$ -particle and  $\gamma$ -ray spectroscopy. A typical Z-distribution is shown in Fig. 1. Rather than exhibiting the expected fusion-fission peak at symmetry, these distributions are absolutely flat for a large central range of Z-values ( $30 \leq Z \leq 75$ ). Near target and projectile Z one observes quite narrow peaks from transfer reactions.

For several bombarding energies the cross section level at symmetry was measured by separating iodine (representing a typical product of the mass-symmetric fission-like reactions). Data evaluation is in progress.

The missing cross section peak at symmetry indicates, that already for  $^{50}\text{Ti} + ^{207}\text{Pb}$  there is a very significant suppression of the fusion channel. This observation is in agreement with the largely suppressed evaporation residue cross sections /1/ in the same reaction at the same energy, which - if reproduced by statistical evaporation calculations - require the assumption of a hindrance factor of about 30 for complete fusion /1/. The cross section deficit is apparently due to the tendency of the system to drift off to symmetric mass splits (quasi fission) and thereby to higher effective fissilities that prevent complete fusion. But also the quasi-fission channel seems to be increasingly hindered as the size of the projectile increases. This is indicated in Fig. 2 where the integral cross sections for quasi fission at the barrier are seen to decrease exponentially. In Fig. 2 this system dependence is compared to the empirical systematics of Armbruster et al. /2/ for the 1n-evaporation residue cross sections measured at the same bombarding energies. The different slopes are consistent with a different scaling of the

extra-push phenomenon for real fusion and quasi fission, respectively.

- /1/ F.P. Heßberger et al., Z. Phys., in press
- /2/ P. Armbruster, Preprint GSI-84-47 (1984)

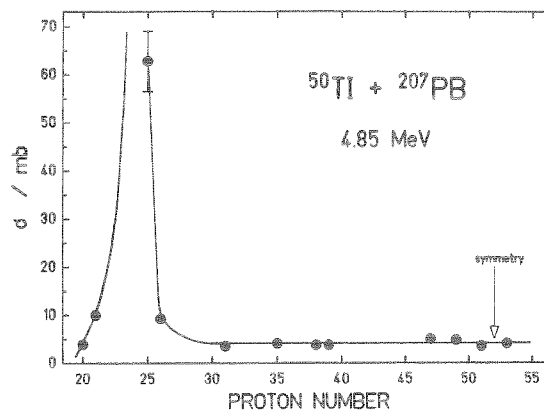


Fig. 1 Element yields for  $^{50}\text{Ti} + ^{207}\text{Pb}$  4.85 MeV

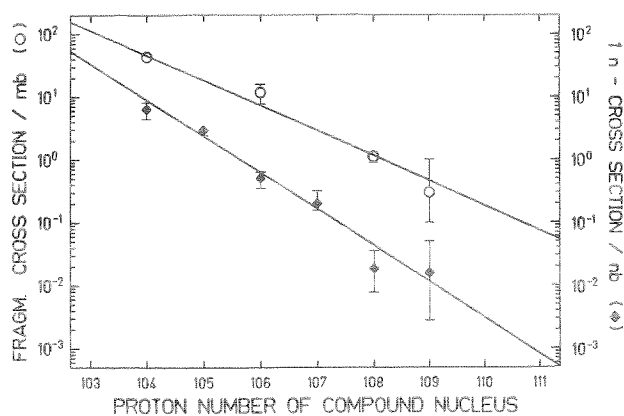


Fig. 2 Quasi fission cross sections (circles) and the 1n-cross sections (diamonds) for production of elements 104 - 109 in  $^{50}\text{Ti}$ ,  $^{54}\text{Cr}$ ,  $^{58}\text{Fe}$  - reactions with  $^{207,208}\text{Pb}$  and  $^{209}\text{Bi}$  - targets. The full lines are least square fits to the data points.

Asymmetric Angular Distributions in Quasi-Fission Reactions

K.Lützenkirchen and J.V.Kratz, Institut für Kernchemie der Universität Mainz

G.Wirth, W.Brüchle, L.Dörr, and K.Sümmerer, GSI Darmstadt

R.Lucas, J.Poitou, and C.Gregoire, DPhN-MF, CEN Saclay

S.Bjørnholm, Niels Bohr Institute, Copenhagen

Recently, there has been much focus on "fusion-fission" angular distributions in heavy systems with unusually large "anisotropies" /1,2/ if compared to expectations based on the transition state theory (TST) and on rotating liquid drop model (RLDM) saddle point shapes. The validity of these expectations for very heavy systems is being questioned /3/ and modifications of the TST /4,5/ are being vividly discussed /6,7/. Deviations from the RLDM expectations are being associated with the onset of quasi-fission reactions /1,2,8,9/ occurring whenever complete fusion is suppressed by dynamical entrance channel limitations /10/.

We have measured differential cross sections  $d^2\sigma/d\Omega dZ$  for quasi-fission fragments from  $^{50}\text{Ti} + ^{208}\text{Pb}$  collisions at 5.0 and 5.5 MeV/A and  $^{56}\text{Fe} + ^{208}\text{Pb}$  collisions at 5.7, 6.1, 6.8, 8.3 MeV/A. The measurements were performed with an off-line X-ray activation technique /11/. Examples for distributions of  $d^2\sigma/d\Omega dZ$  are given in Fig.1. All angular distributions except the ones for  $(Z_1 + Z_2)/2$  are asymmetric around  $\theta_{cm}=90^\circ$  with forward peaking for charges  $Z < (Z_1 + Z_2)/2$  and backward peaking for their heavy complements. These asymmetries decrease as the charge drift from the entrance channel charges progresses toward symmetry. The requirement for the TST to be applicable, i.e. that the system rotates many times as it slowly decays over the barrier, is clearly not met. Because of the vanishingly small fusion cross sections /12/ in the present reactions, we believe that the features displayed by the differential angular distributions in Fig.1 are entirely characteristic of quasi-fission reactions.

The relaxation of rotational degrees of freedom during deep-inelastic collisions has recently been studied in detail /13/. For intermediate reaction times encountered in quasi-fission reactions little is known about the excitation of these modes. In order to extract this information we have fitted the angular distributions for each Z with a simple expression :

$$\frac{d^2\sigma}{d\theta dZ} \propto f(\theta) \sum_{l=0}^{l_m} T_l(2l+1) \int_0^{\theta} \frac{I \cdot \sin \theta \exp(-K^2/2K_0^2)}{\int_0^{\theta} \exp(-K^2/2K_0^2) dK} dK \quad (1)$$

Eqn.1 is based on the factorization of the probability density for a given exit direction into (i) a cross section function  $f(\theta)$  and (ii) a gaussian distribution of projections K of the total angular momentum vector  $l$  on the fission axis with a variance  $K_0^2$ .

(i)  $f(\theta)$  contains the physics of mass equilibration and basically determines the central range of  $d^2\sigma/d\theta dZ$  ( $20^\circ \leq \theta \leq 160^\circ$ ). In Fig.2,  $f(\theta)$  is chosen to be an exponential function describing phenomenologically the statistical decay (during rotation) of an unstable di-nuclear system.

(ii) The cross sections close to the beam axis ( $\theta \leq 20^\circ$ ,  $\theta \geq 160^\circ$ ) reflect the modifications of  $f(\theta)$  by the tilting of the symmetry axis of the di-nuclear system with respect to the reaction plane of the entrance channel.

A fit using eqn.1 with  $l_m=65$   $\hbar$  /9/ and  $T_l=1$  for all  $l$  is shown in Fig.2. For  $^{50}\text{Ti} + ^{208}\text{Pb}$  at 5.5 MeV/A one obtains  $K_0 \approx 7$  ( $K_0 \approx 4.5$  at 5.0 MeV/A) for all near-symmetric charge splits. Theoretically, the equilibrium value for the standard deviation of the tilting fluctuations was estimated /13/ for two spherical nuclei in contact as  $K_0 \approx 14.5$ . This indicates that the tilting mode was not fully relaxed during the reaction time of  $\approx 10^{-20}$  s.

/1/ Back, B. B. et al., Phys. Rev. Lett. 46, 1068 (1981)  
 /2/ Tsang, M. B. et al., Phys. Rev. C 28, 747 (1983)  
 /3/ Plasil, F., Phys. Rev. Lett. 52, 1929 (1984)  
 /4/ Prakash, M. et al., Phys. Rev. Lett. 52, 990 (1984)  
 /5/ Bond, P. D., Phys. Rev. Lett. 52, 414 (1984)  
 /6/ Vandenbosch, R., Phys. Rev. Lett. 53, 1504 (1984)  
 /7/ Bond, P. D., Phys. Rev. Lett. 53, 1505 (1984)  
 /8/ Bock, R. et al., Nucl. Phys. A388, 334 (1982)  
 /9/ Töke, J. et al., Preprint GSI-84-51 (1984)  
 /10/ Bjørnholm, S., Swiatecki, W. J., Nucl. Phys. A391, 471 (1982)  
 /11/ Lucas, R. et al., Z. Phys. A290, 327 (1979)  
 /12/ Hessberger, F. P. et al., submitted to Z. Phys. A, private communication  
 /13/ Døssing, T., Randrup, J., Nucl. Phys. A433, 215 (1985), Nucl. Phys. A433, 280 (1985), and private communication

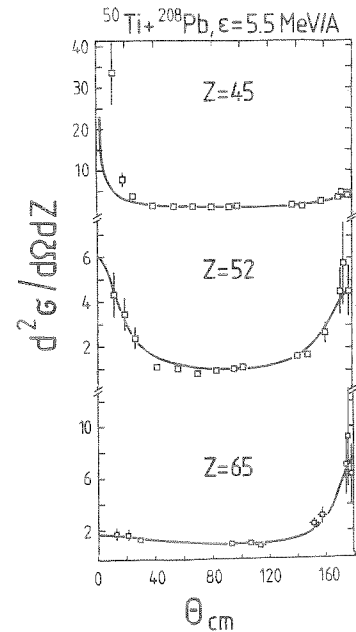


Fig.1:  $d^2\sigma/d\Omega dZ$  for near symmetric charge splits. The solid lines are to visualize the asymmetry with respect to  $90^\circ$ .

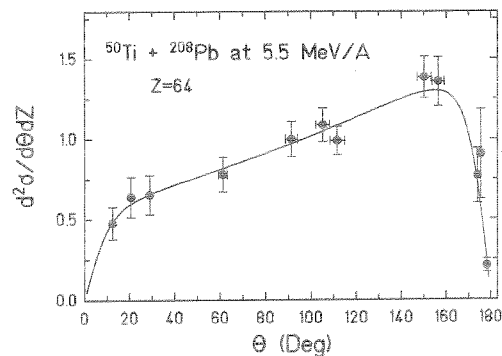


Fig.2:  $d^2\sigma/d\theta dZ$  for Z=64. The solid line is a fit using eqn.1.

SEARCH FOR PIONIC FUSION<sup>B</sup>

Th. Blaich, J. V. Kratz  
Institut für Kernchemie, Universität Mainz, Germany

W. Bröchle, M. Brügger, H. Gäggeler, E. Schimpf  
GSI Darmstadt, Germany

S. M. Qaim  
Institut für Kernphysik, KFA Jülich, Germany

Pionic fusion is a very rare exit channel in nuclear reactions in which all the excitation energy is taken away by a pion while the two nuclei fuse in the ground state or a low-lying, particle-bound excited state of the residual nucleus. This process has been observed in reactions between light nuclei, e.g.  ${}^3\text{He}({}^3\text{He}, \pi^+){}^6\text{Li}$  or  ${}^3\text{He}({}^4\text{He}, \pi^+){}^7\text{Li}$  /1,2/, with total reaction cross sections of  $\approx 100$  nanobarns. With heavier nuclei, the cross sections are expected to be even lower, as the cooperation of all nucleons, required for the transfer of the total excitation energy to a single particle, becomes more and more unlikely. It would, however, be very interesting to find a method sufficiently sensitive to make possible a comparison between the  ${}^{207}\text{Pb}({}^4\text{He}, \pi^-){}^{211}\text{At}$  - and the  ${}^{208}\text{Pb}({}^3\text{He}, \pi^-){}^{211}\text{At}$  - cross sections. There exist qualitative estimates based on a microscopic model of pionic fusion /3/ which predict that the cross section for the pionic fusion of  ${}^{207}\text{Pb}$  and  ${}^4\text{He}$  should be considerably lower than that for  ${}^{208}\text{Pb}$  and  ${}^3\text{He}$ , due to the similarity between entrance and exit channel in the latter case: both consist of a  ${}^{208}\text{Pb}$ -core and three nucleons. Ward et al. investigated the reaction  ${}^{208}\text{Pb}({}^3\text{He}, \pi^-){}^{211}\text{At}$  at several energies and reported cross sections above the pion-production-threshold of several nanobarns /4/. We made an attempt to measure the excitation function of the  ${}^{207}\text{Pb}({}^4\text{He}, \pi^-){}^{211}\text{At}$  - reaction at the isochronous cyclotron JULIC by radiochemical methods. These are best suited for this problem because of their extreme sensitivity: For  $\alpha$ -active nuclei, formation cross sections as low as  $\approx 1$  nanobarn can be measured with an accuracy of  $\approx 10\%$ .

Lead targets fabricated from isotopically enriched material (92.4%  ${}^{207}\text{Pb}$ ) by rolling self-supporting foils of 20 mg/cm<sup>2</sup> were bombarded with  $\alpha$ -particles in a Faraday-cup for about half an hour each with total particle numbers of typically  $4 \cdot 10^{15}$ . In addition, bismuth targets (100  $\mu\text{g}/\text{cm}^2$  supported by foils of 20 mg/cm<sup>2</sup>  ${}^{209}\text{Bi}$ ) were irradiated in order to measure the  ${}^{209}\text{Bi}({}^4\text{He}, xn){}^{213-x}\text{At}$  - cross sections. This was done because the lead targets might potentially contain minute amounts of bismuth impurities. Such a contamination could produce activities comparable to those from pionic fusion due to the very large cross sections ( $\approx$  millibarns). These irradiations lasted about 2 min each, and total particle numbers were typically  $1 \cdot 10^{13}$ .

The formation cross sections of various astatine isotopes were determined by  $\alpha$ -spectroscopy. As the  $\alpha$ -emitters  ${}^{206,208,210}\text{Po}$  are produced via the  ${}^{\text{Bi}}\text{Pb}({}^4\text{He}, xn){}^{\text{Bi}+4-x}\text{Po}$ -reactions in copious quantities, this element had to be removed chemically. In addition, the fission products had to be eliminated in order to suppress an enormous level of  $\beta$ -radiation. To this end the lead and bismuth targets were subjected to chemical separations as described elsewhere /5/ producing weightless At-samples for  $\alpha$ -spectroscopy with chemical yields close to 80%.

From the bismuth irradiations, the excitation functions of the  ${}^{209}\text{Bi}({}^4\text{He}, xn){}^{213-x}\text{At}$  - reactions were extracted, see fig.1. For  $x = 4, 6, 8$  and 10 (products  ${}^{209, 207, 205, 203}\text{At}$  respectively), these behave very much like the excitation functions measured by Djalois et al. for the  $({}^4\text{He}, xn)$  - reactions with  ${}^{197}\text{Au}$  /6/. A new feature are the low values of the  ${}^{209}\text{Bi}({}^4\text{He}, 2n){}^{211}\text{At}$  - cross sections. (The  $({}^4\text{He}, 2n)$  - reaction was not investigated by Djalois et al.) Whereas the excitation functions for  $x = 4, 6, 8$  and 10 drop by a factor of about two for adjacent values of  $x$ , the

$({}^4\text{He}, 2n)$  - cross sections are smaller than those for  $({}^4\text{He}, 4n)$  by a factor of 10.

These cross sections were used to determine by activation techniques the bismuth-contamination of the lead-targets via irradiations below the pion-production-threshold of  $E_{\text{lab}} = 151$  MeV. Then this contribution to the total yield of  ${}^{211}\text{At}$  at energies above the threshold is known and can in principle be subtracted in order to obtain the pionic-fusion-cross section. Unfortunately due to bismuth impurities of the order of several ppm in the  ${}^{207}\text{Pb}$ -targets, we were not able to observe a significant rise of the  ${}^{211}\text{At}$ -production-cross section above the pion threshold, corresponding to an upper limit for the  ${}^{207}\text{Pb}({}^4\text{He}, \pi^-){}^{211}\text{At}$  - cross sections of  $30 \pm 2$  nanobarns. With a cleaner set of targets (enrichment 99.81%, improved target preparation) we anticipate to lower this limit to the 1 nanobarn level in future bombardments.

## References:

1. Le Bornec et al., Phys. Rev. Lett. 47, 1870 (1981)
2. Bimbot et al., Phys. Lett. 114B, 311 (1982)
3. Huber et al., Nucl. Phys. A396, 191c (1983)
4. Ward et al., Indiana University, Dept. of Chemistry and Cyclotron Facility, Ann. Rep. 1980, p. 63
5. Zauner et al., GSI Scientific Report 1983, GSI 84-1, p. 233
6. Djalois et al., Nucl. Phys. A250, 149 (1975)

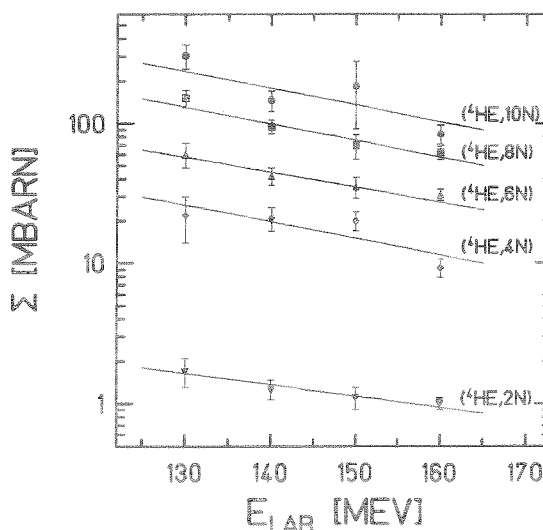
 ${}^{209}\text{Bi}({}^4\text{He}, xn){}^{213-x}\text{At}$ -CROSS SECTIONS

Fig. 1: Excitation functions of the  ${}^{209}\text{Bi}({}^4\text{He}, xn){}^{213-x}\text{At}$  - reactions. The straight lines are drawn to guide the eye.

Search for Volatile Reaction Products in the Reaction  $^{238}\text{U} + ^{238}\text{U}^G$

N. Hildebrand, W. Kieling, J.V. Kratz, N. Trautmann, G. Herrmann\*  
 Institut für Kernchemie, Universität Mainz  
 M. Brügger, H. Gäggeler  
 GSI Darmstadt

Predictions on the chemical behaviour of the super-heavy elements show that the elements 112 (eka-mercury), 114 (eka-lead) and 118 (eka-radon) may be volatile at room temperature. Therefore, chemical procedures for the separation of volatile reaction products were used in various attempts to produce superheavy elements by heavy ion reactions. A few spontaneous fission events have been observed<sup>1,2,3</sup> in the very volatile fractions isolated in the reactions  $^{136}\text{Xe} + ^{238}\text{U}$ ,  $^{238}\text{U} + ^{238}\text{U}$  and  $^{238}\text{U} + ^{248}\text{Cm}$ . But thus far in all experiments only single events could be measured by means of a surface barrier detector. In order to permit a more specific identification of fission fragments by fragment-fragment coincidence measurements a detection system consisting of a cryogenic chamber equipped with an annular surface barrier detector and a solar cell was developed<sup>4</sup>. This equipment has been used in the measurement of volatile reaction products in the reaction  $^{48}\text{Ca} + ^{248}\text{Cm}$ <sup>5</sup>. Furthermore, the system was used in a recent experiment for the detection of very volatile reaction products in the  $^{238}\text{U} + ^{238}\text{U}$  reaction.

In this experiment nine  $^{238}\text{U}$ -targets ( $3.9 \text{ mg/cm}^2$ ) fixed on a rotating target wheel to prevent thermal damage of the targets were bombarded with  $^{238}\text{U}$ -projectiles of 1644 and 1880 MeV energy. The reaction products were transported with a cluster-free argon-jet to the cryo-system. The volatile products were passed first through a quartz tube filled with quartz powder and heated to  $1000^\circ \text{C}$  to trap the non-volatile products and then through a tube filled with tantalum foil ( $T = 800^\circ \text{C}$ ) to remove traces of water. The volatile products were condensed on a solar cell kept at 50 K which operates as a fission fragment detector. With an annular detector in front of the solar cell  $E_1/E_2$  coincident fission fragment measurements and  $\alpha$ -events could be registered. During an irradiation time of 25 h on-line  $\alpha$ -spectra were collected and possible fission events could be listed by a microcomputer system on a line printer. At the end of the irradiation multiscaling experiments were performed to follow the decay of the condensed reaction products.

The main  $\alpha$ -activities can be assigned to radon isotopes and their daughter products. No spontaneous

fission event was observed during the irradiation time of 25 h giving no support for the previous observations.

Figure 1 shows the resulting upper cross section limits for very volatile spontaneously fissioning nuclei versus the half-life on a confidence level of 95 % taking into account a transport time of 30 s in the jet and a deposition and counting efficiency of 10 %.

\*and GSI Darmstadt

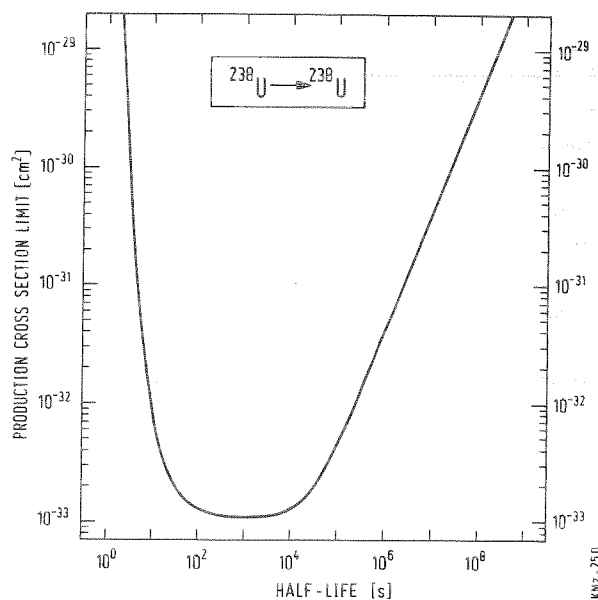


Fig. 1: Cross section limits for the production of volatile spontaneously fissioning products in the reaction  $^{238}\text{U} + ^{238}\text{U}$

#### References

- <sup>1</sup> S. Yashita et al., Lawrence Berkeley Laboratory Report LBL-6547 (1976)
- <sup>2</sup> H. Gäggeler et al., Phys. Rev. Lett. 45, 1824 (1980)
- <sup>3</sup> GSI-Mainz-Livermore Collaboration, to be published
- <sup>4</sup> N. Hildebrand et al., GSI Scientific Report 1982, 83-1, 234 (1983)
- <sup>5</sup> N. Hildebrand et al., GSI Scientific Report 1983, 84-1, 84 (1984)

Transfer Yields of Fm through Lr Isotopes from Reactions with  $^{254}\text{Es}$

M. Schädel, W. Brüchele, M. Brügger, H. Gäggeler, K. J. Moody, D. Schardt, K. Sümmerer  
GSI Darmstadt

E.K. Hulet, A.D. Dougan, R.J. Dougan, J.H. Landrum, R.W. Lougheed, J.F. Wild  
LLNL Livermore, CA

G.D. O'Kelley  
ORNL Oak Ridge, TN

Previously we reported experiments with 101 MeV  $^{16}\text{O}$ , 98 MeV  $^{18}\text{O}$  and 127 MeV  $^{22}\text{Ne}$  projectiles on  $^{254}\text{Es}$  as a target<sup>1</sup>. From these experiments we have obtained formation cross sections for trans-einsteinium isotopes which are shown in Fig. 1. The curves shown are Gaussian with a FWHM = 2.25 u. The most interesting point to note is the high cross sections, especially in comparison with other possible reactions leading to the same product. Peak cross sections of about 1 mb for Md compare with only 1  $\mu\text{b}$  in  $^{18}\text{O} + ^{249}\text{Cf}$  [2] and 10 nb in  $^{18}\text{O}, ^{22}\text{Ne} + ^{248}\text{Cm}$  [3]. The neutron-rich isotope  $^{260}\text{Lr}$  is produced with 1.1  $\mu\text{b}$  in the  $^{22}\text{Ne} + ^{254}\text{Es}$  transfer reaction, while the compound nuclear reaction  $^{248}\text{Cm}(^{15}\text{N}, 3n)^{260}\text{Lr}$  gives a cross section of only 2 nb [4]. These higher cross sections with  $^{254}\text{Es}$  targets can easily be understood when one keeps in mind that for systems with light projectiles and heavy targets at barrier energies (i) about 50% of the total reaction cross section goes into transfer channels, (ii) transfer products heavier than the target are formed predominantly, and, most important, (iii) because of negative  $Q_{\text{gg}}$ -values these primary fragments are formed with very low excitation energies ( $\leq 10$  MeV), so that in most cases the observed products are directly formed or stem from a one-neutron evaporation channel.

An interesting systematic feature, which is most pronounced with  $^{18}\text{O}$  as a projectile (see Fig. 1), is the observation of equally high cross sections for the 1p (Fm)- and the 2p (Md)-transfer followed by a large gap of two to three orders of magnitude and then again only slightly higher cross sections for the 3p (No)- over the 4p (Lr)-transfer. We interpret this as a structural effect in the light projectile, since it is not observed if the same transfer channels are studied in the  $^{238}\text{U} + ^{238}\text{U}$  or  $^{238}\text{U} + ^{248}\text{Cm}$  reactions.

From the isotope distributions shown in Fig. 1 we are able to predict cross sections of yet unknown heavy actinide nuclides. The nuclides  $^{260}\text{Md}$ ,  $^{260}\text{No}$  and  $^{261}\text{Lr}$  should be produced with cross-sections between 100 nb and 1  $\mu\text{b}$ . For  $^{261}\text{No}$  and  $^{262}\text{Lr}$  we predict several tens of nb, whereas the extrapolation to  $^{261}\text{Md}$ ,  $^{262}\text{No}$  and  $^{263}\text{Lr}$  yield a maximum of a few nb.

References

1. K. Sümmerer et al., Proc. XXII Int. Winter Meeting on Nuclear Physics, Bormio, 1984, p. 513, M. Schädel et al., GSI Scientific Report 1983, GSI 84-1, p. 78, and references therein.
2. D. Lee et al., Phys. Rev. **C27**, 2656 (1983)
3. D. Lee et al., Phys. Rev. **C25**, 286 (1982)
4. K. Eskola et al., Phys. Rev. **C4**, 632 (1971)

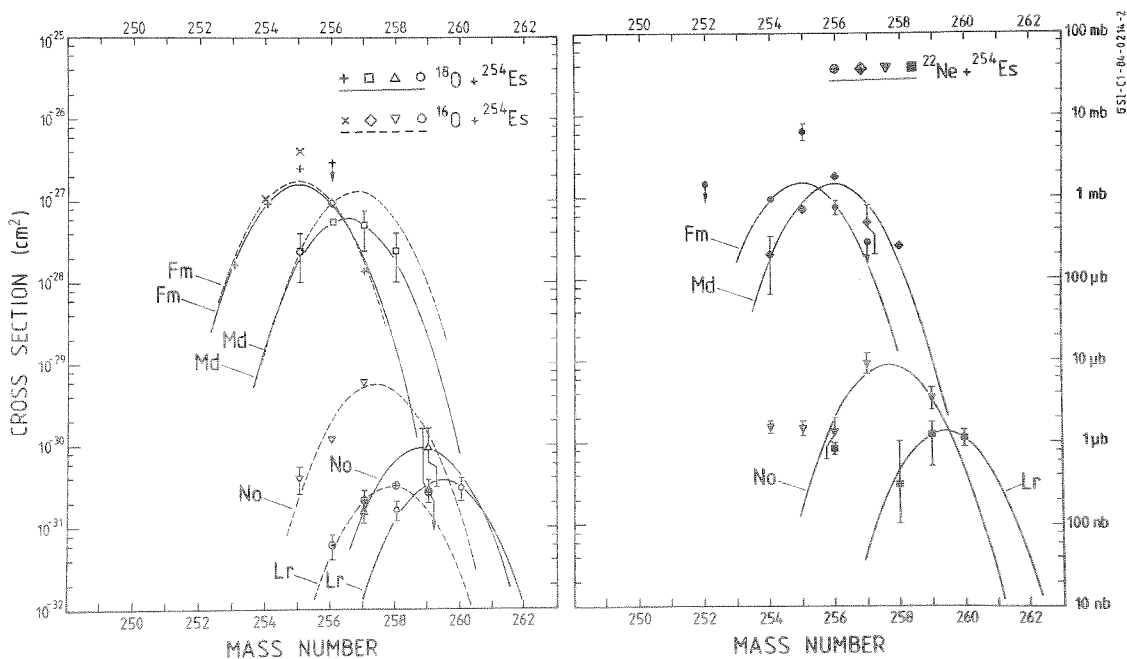


Fig. 1. Isotopic distributions measured for 101 MeV  $^{16}\text{O}$  and 98 MeV  $^{18}\text{O}$  (left) and for 127 MeV  $^{22}\text{Ne}$  (right) on  $^{254}\text{Es}$ .

Excitation Functions for Heavy Actinides from the Reaction of  $^{40}\text{Ca}$  with  $^{248}\text{Cm}$ <sup>B</sup>

M.M. Fowler, W.R. Daniels, D.C. Hoffman  
Los Alamos National Laboratory

W. Bröchle, M. Brügger, H. Gäggeler\*, M. Schädel, K. Sümmerer, G. Wirth  
GSI-Darmstadt

T. Blaich, G. Herrmann†, J.V. Kratz, M. Lerch, N. Trautmann  
Universität Mainz

D. Lee, K.J. Moody, G.T. Seaborg  
Lawrence Berkeley National Laboratory

H.R. von Gunten  
Universität Bern and EIR Würenlingen

In the previous annual report we presented<sup>1</sup> excitation functions for heavy actinides from the reaction of  $^{48}\text{Ca} + ^{248}\text{Cm}$ . These investigations have been extended to the system  $^{40}\text{Ca} + ^{248}\text{Cm}$  to explore the influence of the very different N/Z-ratios between  $^{40}\text{Ca}$  and  $^{48}\text{Ca}$  on the production of heavy target-like products. All experimental details are described in Ref. 1. The  $^{248}\text{Cm}$  target (1.7 mg/cm<sup>2</sup> of  $^{248}\text{Cm}$ ) was irradiated with  $E_{\text{lab.}} = 235, 260$  and  $259$  MeV  $^{40}\text{Ca}$  projectiles. These energies correspond to 1.01, 1.10 and 1.25 times the calculated interaction barrier. The energy loss within the target was measured to be 14 MeV.

The evaluated cross sections for the production of isotopes of Bk, Cf, Es and Fm are listed in Table 1. Independent of the bombarding energy, the mass distributions peak at the most probable mass numbers  $A_p$  of about 248 (Bk), 248 (Cf), 250 (Es) and 252 (Fm), which correspond to net transfers of (+1p, -1n), (+2p, -2n), (+3p, -1n) and (+4p, 0n) nucleons from the projectile to the target. It is interesting to note that these isotopes are very near to N=152 (and complementary light products near N=20) which might indicate the influence of shell effects on these transfer reactions. Moreover, these  $A_p$  values are surprisingly neutron-rich compared to calculated primary  $A_p^1$  values obtained on the basis of potential energy considerations<sup>2</sup> which give 242 (Bk), 244 (Cf), 247 (Es) and 250 (Fm).

In Fig. 1 are plotted excitation functions for the elements Bk through Fm which are determined from Gaussian shaped isotope yield curves. We observe highest cross sections for the lowest (mainly sub-barrier) energy and rather constant or slowly decreasing values for the higher energies. However, since reaction products were collected at forward angles only ( $\theta \leq 60^\circ$ ), it cannot entirely be excluded that part of the target-like nuclides were lost at the highest bombarding energy because of an emission angle  $\geq 60^\circ$ .

\* presently at EIR Würenlingen  
† also at GSI Darmstadt

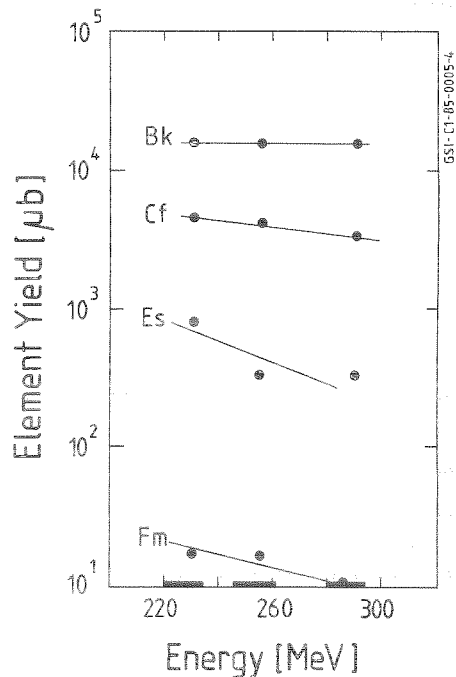
1 W.R. Daniels et al., GSI Sci. Rep. 1983, p. 85.  
2 H. Freiesleben and J.V. Kratz, Phys. Rep. 106, 1(1984).

Table 1: Cross sections for the production of heavy actinides in the bombardment of  $^{248}\text{Cm}$  with  $^{40}\text{Ca}$  at different energies.

	(221 - 234) MeV <sup>a</sup>		(246 - 259) MeV <sup>a</sup>		(281 - 294) MeV <sup>a</sup>	
	$\sigma$ ( $\mu\text{b}$ )	$s^b$ (%)	$\sigma$ ( $\mu\text{b}$ )	$s^b$ (%)	$\sigma$ ( $\mu\text{b}$ )	$s^b$ (%)
Bk 244	64.7	20	60.0	5	47.3	9
245	675	12	605	5		
246	2020	4	1900	2		
<sup>248</sup> Cm	5470	6	4575	3		
250	250	8	330	8		
Cf 245	84.7	14	44.2	14		
246	215	5	185	19	135	2
248	1800	5	1585	2	1375	3
250	320	63	250	53	175	80
252	50	82	45	65	40	80
Es 249 <sup>g</sup>	150	7			80	7
250	190	26	145	20	150	10
252	12.8	23	10.9	37	6.6	30
253	2.6	20	2.5	40	1.8	40
254m	0.33	33	0.30	20	0.25	32
Fm 250			2.8	14		
251	7.0	80	5.2	21		
252	6.85	2	5.2	8	3.3	12
254	0.39	30	0.31	6	0.22	9
256	0.004	50	0.007	30		

<sup>a</sup> Range of projectile energy (laboratory system) in target.  
<sup>b</sup> Statistical standard deviation based on the analysis of the decay data.

Fig. 1: Excitation functions for target-like transfer elements from  $^{40}\text{Ca} + ^{248}\text{Cm}$ .



Cold massive transfer in the reaction  $^{48}\text{Ca} + ^{248}\text{Cm}^B$

H. Gäggeler\*, W. Bröchle, M. Brügger, M. Schädel, K. Sümmerer, G. Wirth  
GSI Darmstadt

M. Lerch, Th. Blaich, G. Herrmann†, N. Hildebrand, J.V. Kratz, N. Trautmann  
Universität Mainz

K.E. Gregorich, K.J. Moody, G.T. Seaborg  
Lawrence Berkeley National Laboratory

H.R. von Gunten  
EIR Würenlingen

D.C. Hoffman×, M.M. Fowler, W.R. Daniels  
Los Alamos National Laboratory

In the reaction  $^{48}\text{Ca} + ^{248}\text{Cm}$  qualitative evidence indicated that far-below target nuclides are produced already at near-barrier energies with remarkably high cross sections<sup>1</sup>. On the other hand, a steep decrease in cross sections was found for heavy transcurium elements<sup>2</sup>. To quantify the above mentioned observation we have determined isotope yields for the elements Rn through Pu using radiochemical techniques. A 1.7 mg/cm<sup>2</sup> thick  $^{248}\text{Cm}$  (oxide) target was bombarded by  $^{48}\text{Ca}$  at  $E_{\text{lab}} = 264$  MeV. The measured energy loss within the target was 16 MeV. U, Np and Pu yields were determined off-line: Copper catcher foils (about 6 mg/cm<sup>2</sup>) placed behind the target were chemically processed after bombardment and final samples analysed for alpha and gamma activities. Yields for short-lived  $\alpha$ -active isotopes of Rn, Ra, Ac and Th were measured on-line by coupling a gas-jet transportation system to a cryogenic chamber or the ROMA apparatus<sup>3</sup>.

Evaluated cross sections together with values for trans-curium yields<sup>2</sup> are plotted in Fig. 1. We observe a very asymmetric shape of the mass yield curve with rather constant cross sections of about 200  $\mu\text{b}$  for  $^{216}\text{Rn}$ ,  $^{222}\text{Ra}$ ,  $^{225}\text{Ac}$ , and  $^{228}\text{Th}$  (maximum isotope yields of the corresponding elements). In addition, isotope yield curves are much broader for below Cm elements (i.e. FWHM = 5 amu for Rn) compared to above Cm elements (i.e. FWHM = 2.5 amu for Fm).

In order to estimate average excitation energies for surviving products, in Table I the measured maxima  $A_p$  of the Gaussian isotope yield curves from Fig. 1 are compared with calculated primary  $A'_p$  values deduced from potential energy considerations<sup>4</sup>. The differences  $\Delta A = A'_p - A_p$  give a crude estimate of the number of neutrons evaporated. Even for the far below Cm element Rn (transfer of 10 protons and about 22 neutrons from the target to the projectile)  $\Delta A$  is 1.5 amu corresponding to an excitation energy of about 15 to 20 MeV only. It is interesting to note that complementary projectile-like fragments are rather neutron-rich isotopes, i.e. such nuclides like  $^{65}\text{Fe}$ ,  $^{66}\text{Co}$  or  $^{72}\text{Ni}$  should be produced at a 200  $\mu\text{b}$  level in this reaction.

A similar investigation made in a bombardment of the same target by 259 MeV  $^{40}\text{Ca}$  projectiles revealed that

trans-curium element yields are enhanced<sup>2</sup> whereas sub-curium element yields are considerably lower compared to  $^{48}\text{Ca}$ , i.e. the cold massive nucleon transfer towards mass symmetry is no longer evident for  $^{48}\text{Ca} + ^{248}\text{Cm}$ .

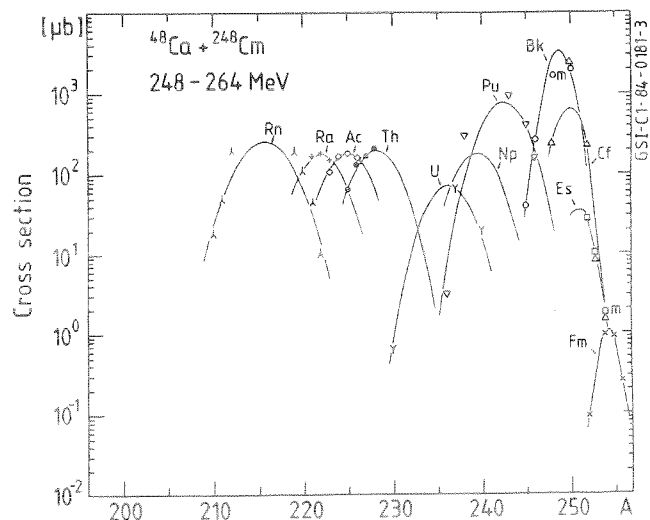
- \* presently at EIR Würenlingen
- † also at GSI Darmstadt
- × presently at LBL Berkeley

1. P. Armbruster et al., GSI-Scientific Report 1983, p. 81 (1984)
2. D.C. Hoffman et al., submitted to Phys. Rev. C. (1984)
3. K. Sümmerer et al., Preprint GSI-84-17
4. H. Freiesleben and J.V. Kratz, Phys. Rep. 106,1 (1984)

Table I: Differences between primary ( $A'_p$ ) and secondary ( $A_p$ ) most probable masses

Element	$A_p$	$A'_p$	$\Delta A$
Fm (Z = 100)	254.5	254.75	+ 0.25
Cf ( 98 )	250.0	250.25	+ 0.25
Pu ( 94 )	242.5	242.25	- 0.25
U ( 92 )	236.0	236.50	+ 0.50
Th ( 90 )	228.5	230.50	+ 2.00
Ra ( 88 )	221.75	223.25	+ 1.50
Rn ( 86 )	215.5	217.00	+ 1.50

Fig.1 : Radiochemically determined isotope yields for Rn through Fm from  $^{48}\text{Ca} + ^{248}\text{Cm}$





New nuclide  $^{243}\text{Np}$ , and tentative identification of  $^{244}\text{Np}$

K. J. Moody, W. Brüche, M. Brügger, H. Gäggeler\*, G. Herrmann\*,  
 M. Schädel, K. Sümmerer (GSI Darmstadt)  
 N. Kaffrell, J. V. Kratz, J. Rogowski, R. Schmoll,  
 H. Tetzlaff, N. Trautmann (Univ. Mainz)  
 M. M. Fowler (LANL), J. Alstad (Univ. Oslo)  
 M. Skalberg, G. Skarnemark (Univ. Göteborg)  
 H. R. von Gunten, A. Türler (Univ. Bern)  
 D. C. Hoffman (LBL)

Neutron-rich neptunium isotopes are produced with high yield in the  $^{136}\text{Xe} + ^{244}\text{Pu}$  reaction<sup>1</sup>. We have used automated chemistry techniques coupled with a gas jet transportation system to isolate new neptunium isotopes from a mixture of recoiling reaction products.

In one experiment, the coupled centrifuge system, SISAK<sup>2</sup>, was used to isolate neptunium with a reduction-oxidation procedure on the time scale of a few seconds. Activity from the gas jet was continuously processed by SISAK, which produced a contaminant-free sample that continuously flowed in front of a gamma ray detector. In addition to the gamma rays of the known  $^{242}\text{B}^{242}\text{Np}$  activity, we observed gamma lines at 287.5 and 162.8 keV, which may correspond to the  $5/2^+ [622] \rightarrow 7/2^+ [624]$  transition in  $^{243}\text{Pu}$  (figure 1) and the  $6^+ \rightarrow 4^+$  transition in the ground state rotational band of  $^{244}\text{Pu}$ , respectively. Both initial levels are likely to be populated in the beta decays of  $^{243}\text{Np}$  (probable ground state  $J^\pi = 5/2^+ [642]$ ) and  $^{244}\text{Np}$  (probably coupled from  $p\ 5/2 [642]$  and  $n\ 9/2 [734]$  to  $J^\pi = 7^-$ ). Initial half life estimates from the SISAK experiments were 50 seconds for  $^{243}\text{Np}$  and 20 seconds for  $^{244}\text{Np}$ , in comparison with predicted values from the microscopic theory<sup>3</sup> of 195 seconds and 8 seconds, respectively, and with those from the gross theory<sup>4</sup> of 25 minutes and 3 minutes, respectively.

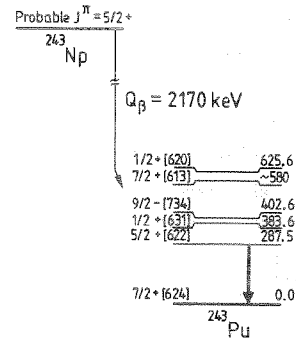
In an effort to better define the half life of  $^{243}\text{Np}$ , an experiment was performed with the Automated Rapid Chemistry Apparatus, ARCA<sup>5</sup>. Activity from the gas jet was collected batchwise and processed to produce a neptunium fraction in 2.8 minutes. Samples contained small contaminants of Hf, La and Ce, which did not interfere with the determination of the half life of the 287.5 keV gamma ray activity. The decay of each sample was followed for several half lives; the data from sixteen runs were combined, resulting in the decay curve shown in figure 2.

As a further verification of the identity of  $^{243}\text{Np}$ , the initial activity of the 287.5 keV gamma line was converted to a cross section. A total decay energy of 2170 keV is known<sup>6</sup> for the  $\beta^-$  decay of  $^{243}\text{Np}$ . Log ft values for  $\beta^-$  decays to the levels in  $^{243}\text{Pu}$  were assumed to be equal to those for equivalent decays orig-

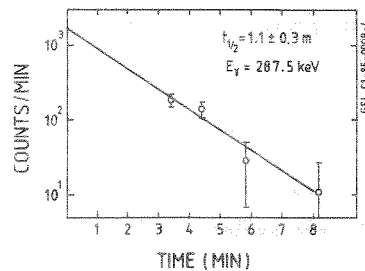
inating from  $^{239}\text{Np}$ . Approximately 70% of the decays pass through the  $5/2^+$  state at 287.5 keV. The internal conversion coefficient for an M1 transition was estimated, yielding an overall gamma ray intensity of roughly 30%. This results in a cross section of 20 mb, consistent with estimates<sup>1</sup> based on the systematics of the yields of other actinides produced in the reaction.

\* and Universität Mainz  
 \* presently at EIR Würenlingen

1. K. J. Moody et al., this Report.
2. H. Tetzlaff et al., this Report.
3. H. V. Klapdor et al., At. Data Nucl. Data Tables 31, 81 (1984).
4. K. Takahashi et al., At. Data Nucl. Data Tables 12, 101 (1973).
5. W. Brüche et al., GSI Scientific Report 1983, GSI 84-1.
6. E. R. Flynn et al., Phys. Rev. C19, 355 (1979).



1. Proposed decay of  $^{243}\text{Np}$ . The observed photon transition is indicated.



2. Least-squares fit to the half life of  $^{243}\text{Np}$ .

Light actinide yields from the reaction of  $^{136}\text{Xe}$  with  $^{244}\text{Pu}$

K. J. Moody, W. Bröchle, M. Brügger, H. Gäggeler\*, G. Herrmann\*,  
 M. Schädel, K. Sümmerer (GSI Darmstadt)  
 N. Kaffrell, J. V. Kratz, J. Rogowski, R. Schmoll,  
 H. Tetzlaff, N. Trautmann (Univ. Mainz)  
 M. M. Fowler (LANL), J. Alstad (Univ. Oslo)  
 M. Skalberg, G. Skarnemark (Univ. Göteborg)  
 H. R. von Gunten, A. Türler (Univ. Bern)  
 D. C. Hoffman (LBL)

We are studying the  $^{136}\text{Xe} + ^{244}\text{Pu}$  reaction to assess the possibility of producing new, neutron-rich isotopes of the light actinides. A target of  $^{244}\text{Pu}$  (1 mg/cm<sup>2</sup>) was irradiated with  $^{136}\text{Xe}$  ions at an energy between 750 and 860 MeV (1.05 to 1.20 times the nominal Coulomb barrier). Recoiling reaction products were stopped in a volume of Ar gas containing KCl clusters, and were transported along a capillary to an Automated Rapid Chemistry Apparatus (ARCA)<sup>1</sup>, where they were collected on a glass frit. The elements from Pa (Z=91) to Pu (Z=94) were chemically separated; the resultant fractions were ready for gamma-ray counting between 4 and 9 minutes after the end of each accumulation. Data from twelve runs were summed to improve statistics. An overall chemical yield and transportation efficiency of 25% and a transportation time of 60 seconds are assumed in the cross section calculations.

Cross sections are plotted against product mass number in figure 1. Where necessary, cross sections have been corrected for feeding prior to the chemical separation, except for the  $^{243}\text{Pu}$  point. Data given for  $^{242}\text{Np}$  and  $^{240}\text{Np}$  are the sums of the cross sections of both isomeric states; the isomer ratios are roughly 1. Only the high spin isomer of  $^{234}\text{Pa}$  was determined. We estimate from our data that, in this reaction, the cross sections for the production of hitherto undiscovered  $^{243}\text{Np}$  and  $^{241}\text{U}$  are 15 mb and 3 mb, respectively. We also expect cross sections in excess of 1 mb for  $^{244}\text{Np}$  and  $^{243}\text{U}$ .

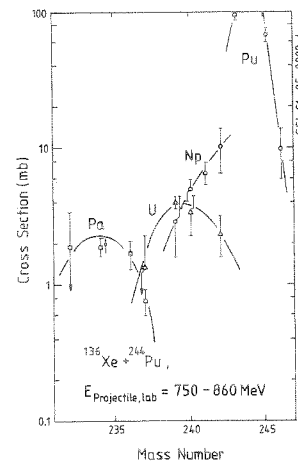
Our data does not agree with that from a previous study of the  $^{136}\text{Xe} + ^{244}\text{Pu}$  system<sup>2</sup>. We attribute this to contaminants in the chemical fractions in the previous work, which interfered with cross section determinations via gross beta activity. Figure 2 shows a comparison of our data with that from the  $^{136}\text{Xe} + ^{248}\text{Cm}$  system<sup>3</sup>. The differences in the absolute magnitudes of the cross section distributions for similar exchanges with the different targets is more due to the reaction energies than to  $\Gamma_n/\Gamma_f$  considerations. Comparison of the two systems shows a slight enhancement of neutron-deficient yields from the  $^{136}\text{Xe} + ^{244}\text{Pu}$  reaction relative to those from the  $^{136}\text{Xe} + ^{248}\text{Cm}$  reaction. This can be explained in terms of differences

in the potential energy surfaces of the two reactions; for a given exchange of charge, minimum potential energy exchanges result in below-target actinide products from  $^{244}\text{Pu}$  with one less neutron than those produced from  $^{248}\text{Cm}$ .

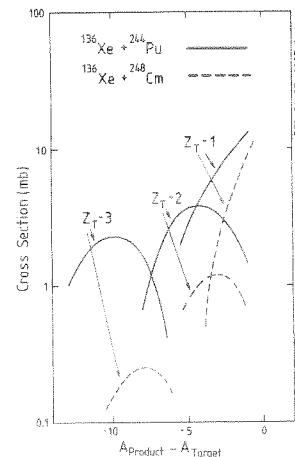
\* and Universität Mainz

\* presently at EIR Würenlingen

1. W. Bröchle et. al., GSI Scientific Report 1983, GSI 84-1.
2. D. Lee et. al., LBL Nuclear Science Division Annual Report 1978-79, LBL-9711.
3. K. Moody, LBL Report LBL-16249 (1983).



1. Light actinide yields from  $^{136}\text{Xe} + ^{244}\text{Pu}$ . A 25% efficiency is assumed.



2. Comparison of actinide yields from 750-860 MeV  $^{136}\text{Xe} + ^{244}\text{Pu}$  with those from 700-790 MeV  $^{136}\text{Xe} + ^{248}\text{Cm}$ .  $Z_T$  is the target proton number.

Production of below-target products in  $^{136}\text{Xe}$  induced reactions

A. Türler\*, H. Gäggeler\*, H.R. von Gunten\*\*\*, F. Wegmüller\*  
 \*Universität Bern, \*\*E.I.R. Würenlingen

R. Schmoll, J.V. Kratz, H. Keller, S. Zauner  
 Institut für Kernchemie, Universität Mainz

K.J. Moody, W. Bröchle, M. Brügger, M. Schädel, K. Sümmerer, G. Wirth  
 GSI Darmstadt

Quasielastic transfer reactions induced by  $^{136}\text{Xe}$  on  $^{239,244}\text{Pu}$ ,  $^{238}\text{U}$ -targets were used to produce below-target isotopes. The excitation functions for these reactions have to be known for the optimization of the bombarding energies for the production of new neutron-rich light actinide nuclides /1/. Furthermore, a comparison of actinide excitation functions with those for the much less fissile transfer products from  $^{136}\text{Xe} + ^{186}\text{W}$  reactions will shed some light on the sensitivity of products populated by transfer channels to fission and neutron emission. The experimental techniques involved collection of the target-like recoils in several Cu-catcher foils, radiochemical separations and  $\alpha$ -activity measurements.

The catcher foils from the  $^{239,244}\text{Pu}$  and the  $^{238}\text{U}$  target irradiations were dissolved in a mixture of hot conc.  $\text{HNO}_3$  and traces of  $\text{HClO}_4$ . The solution was passed through a 60x3 mm CIX-column in the nitrate form; the Pa/Th-fraction was eluted with 9m  $\text{HCl}/0.1\text{m HF}$ , the Np/Pu-fraction with 6m  $\text{HCl}/3\% \text{NH}_2\text{OH}\cdot\text{HCl}/2\% \text{NH}_4\text{J}$  and 4.5m  $\text{HCl}$ , the U-fraction with 0.5m  $\text{HCl}$ . The Pa/Th- and the U-fractions were purified by solvent extractions. Chemical yields were determined with radiotracers. The catcher foils from the  $^{186}\text{W}$  irradiations were dissolved in a mixture of conc.  $\text{HNO}_3$  and  $\text{H}_2\text{O}_2$ . Hf and Lu were extracted into TBP absorbed on Voltalef powder and backextracted with 2m  $\text{HCl}/\text{H}_2\text{O}_2$ . The Ta-fraction which passed through the TBP-column was purified and coprecipitated with  $\text{Fe}(\text{OH})_3$ . Hf and Lu were separated from each other on a HDEHP-column and coprecipitated with  $\text{Fe}(\text{OH})_3$ .

Preliminary results for the bombardment of  $^{238}\text{U}$  and  $^{244}\text{Pu}$  targets ( $700\text{-}900 \mu\text{g}/\text{cm}^2$ ) with  $^{136}\text{Xe}$  in the energy range  $(1.1\text{-}1.2) \cdot E_B$  are shown Fig.1. For one-neutron transfers to and from the target and also for two-proton transfers from the target quite similar cross sections are observed independent of the target nuclide. In addition, isotope yields do not significantly decrease for lower masses. This indicates that products are formed in a broad range of excitation energies. Similar observations are made for transfer reactions between  $^{136}\text{Xe}$  and  $^{186}\text{W}$ . A preliminary excitation function for the  $^{186}\text{W}(^{136}\text{Xe}, ^{138}\text{Ba})^{184}\text{Hf}$ - reaction is shown in Fig.2. The excitation function exhibits the typical features of quasielastic transfer reactions /2/: a sharp increase at the interaction barrier /3/, and a behaviour

consistent with a constant cross section at energies above the barrier. This is expected /2/ because maximal transfer probabilities occur at the same range of interaction radii at all energies. The cross section at  $E_{\text{CM}}=642 \text{ MeV}$  represents a lower limit because of kinematic losses which may not have been fully corrected.

The processing of the data of the bombardments on the  $^{239}\text{Pu}$ -target is in progress.

References

- /1/ For details see K.J.Moody et al., this report
- /2/ D.Gardes et al., Phys.Rev. C18, 1298 (1978)
- /3/ G.Franz et al., Z. Physik A291, 167 (1979)

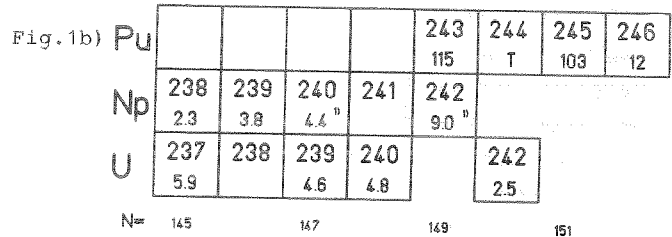
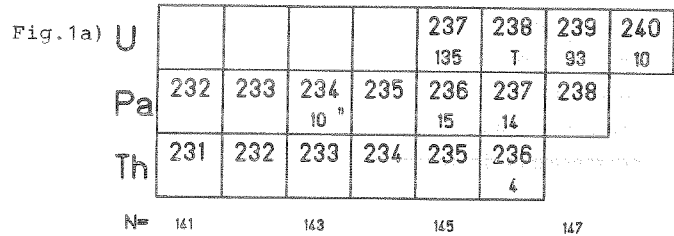


Fig.2)

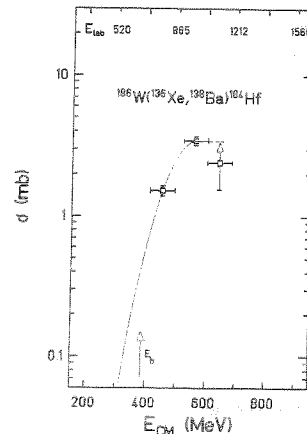


Fig.1a): Section of the chart of nuclides indicating relative cross sections in mb for  $^{136}\text{Xe}$  induced reactions on  $^{238}\text{U}$ . (Estimated target thickness of  $700 \mu\text{g}/\text{cm}^2$ ).

Fig.1b): Section of the chart of nuclides indicating absolute cross sections in mb for  $^{136}\text{Xe}$  induced reactions on  $^{244}\text{Pu}$ . (values for Pu isotopes are only relative, chemical yield is estimated to be 50%). Typical errors of all values are about +/- 25%.

1) Cross sections only for ground state nuclides.

Fig.2 : Energy dependence for two-proton stripping from  $^{186}\text{W}$ .

Rapid Preparation of Lanthanide and Actinide Samples by Vacuum Evaporation<sup>G</sup>

C. Frink, W. Kieling, N. Trautmann, G. Herrmann\*

Institut für Kernchemie, Universität Mainz

E. Jäger, M. Schädel, E. Schimpf

GSI Darmstadt

As a consequence of the small production cross sections and the relatively short half-lives of neutron-rich actinide nuclides produced in heavy-ion reactions with actinide targets an almost quantitative and fast procedure is needed for the preparation of thin and uniform samples for  $\alpha$ - and spontaneous fission measurements from chemically separated fractions of individual elements. Such samples can be obtained by vacuum evaporation of actinide compounds with low evaporation heat<sup>1</sup> from hot titanium surfaces<sup>1,2</sup>. We have investigated the optimal conditions for an adaption of this technique to the automated rapid chemistry apparatus ARCA<sup>3</sup> by using europium as a model element for the heavier actinides.

Fig. 1 shows the automated vacuum evaporation system which was developed in these experiments. The eluate passing through the capillary (4) of the chromatographic column is evaporated to dryness by heating the crucible and blowing hot helium through the nozzle (5). The nozzle is placed in such a way above the crucible that the eluate is fixed in the centre of the crucible by the outstreaming hot helium. Then, the titanium crucible is transported pneumatically by means of a cylinder from the evaporation chamber to the high vacuum chamber where evaporation from the hot titanium surface takes place. For counting, the collector foil (6) can be transported pneumatically out of the high vacuum chamber.

All experiments were carried out with <sup>152</sup>Eu activity. To simulate the conditions in the ARCA system the activity was dissolved in 3 ml 1 M HCl and passed through an anion exchange column into the titanium crucible which has a capacity of about 180  $\mu$ l. At a pressure of 700 mbar in the evaporation chamber 85 % and 60 % of the eluated activity were found in the crucible at flow-rates of 0.25 and 0.7 ml/min, respectively. Helium gas with a temperature of  $\approx$  220° C and a crucible temperature as obtained by 100 - 170 V heating voltage were required. At lower pressures the yield decreased.

In order to find out the best conditions for the evaporation step in the high vacuum chamber 10  $\mu$ l of the <sup>152</sup>Eu-solution were first evaporated to dryness in the titanium crucible and then volatilized at a pressure of  $6 \cdot 10^{-5}$  mbar. The crucible temperature

was varied from 1280 - 1350° C and the evaporation time from 20-90 s. At an evaporation time of 90 s and a temperature of 1280° C, 20 % of the activity remained in the crucible whereas at 1350° C and 60 s evaporation time only 5 - 8 % could be found. The best collection yields ( $\approx$  50 %) were obtained at a crucible-foil distance of 10 mm.

\*and GSI Darmstadt

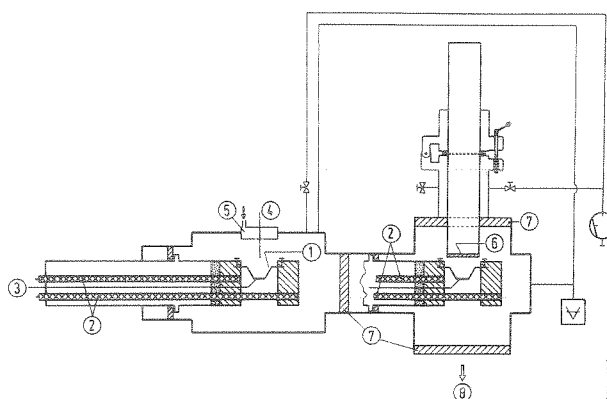


Fig. 1: Vacuum evaporation system showing the two positions of the evaporation crucible (1) during the eluate collection and during the lanthanide evaporation step. 1 titanium-crucible; 2 resistance heating; 3 thermo-couple; 4 capillary from chromatographic column; 5 helium nozzle; 6 catcher foil; 7 slide valves; 8 to vacuum pump

#### References

- <sup>1</sup>E. Rhede et al., Zentralinstitut für Kernforschung Rossendorf, Bericht ZfK 367 (1978) S. 23
- <sup>2</sup>C. Frink et al., GSI Scientific Report 1982, 82-1, 219 (1983)
- <sup>3</sup>W. Brüche, M. Brügger, B. Haefner, M. Schädel, E. Schimpf, GSI Scientific Report 1983, 84-1, 247 (1984)

### Rapid Gaschromatographic Separation of Lanthanide-Hexafluoroacetylacetonates<sup>G</sup>

N. Greulich, U. Hickmann, N. Trautmann, G. Herrmann\*  
 Institut für Kernchemie, Universität Mainz

For the development of fast separation techniques for transplutonium elements homologue lanthanides can be used because of the great similarities of their chemical and physical properties at the same oxidation states. Radioactive lanthanide isotopes are easily obtained either by neutron activation or from fission-product mixtures of <sup>235</sup>U. Thus, experimental problems concerning  $\alpha$ -measurements as required for the heavier actinides are avoided during the development of a separation method. In this work, a fast method for unravelling lanthanide element mixtures in form of their hexafluoroacetylacetonates using gaschromatography is described.

Hexafluoroacetylacetonates of lanthanide elements were synthesized with a liquid-solid extraction method<sup>1</sup>, modified to the experimental conditions for the preparation of mixed ligand complexes of lanthanides with hexafluoroacetylacetone (HFA) and tri-octylphosphine oxide (TOPO) as a donoractive compound<sup>2</sup>. The isolation of the lanthanide elements as a group from the fission product mixture can be performed within 9 s, as could be demonstrated by the  $\gamma$ -spectroscopic identification of lanthanide isotopes with half-lives in the range of some seconds.

During this group separation, the mixed ligand complexes of the type  $\text{Ln}(\text{HFA})_3 \cdot 2\text{TOPO}$  are fixed in a small trap on a fine grained carrier, e.g. Chromosorb. This column is placed in the injector of a gaschromatograph<sup>3</sup> and heated up to 240° C. Nitrogen saturated at 60° C with HFA is fed in with a flow rate of 30 ml/min, flushing the volatilized complexes into the separation column (glass column, 2 m long by 2.4 mm inner diameter, stationary phase Chromosorb W, 100-120 mesh, with 3 % Dexsil 300 GC). The gaschromatographic oven is temperature-programmed between 150 °C and 220 °C with a constant rate of 8 °C/min.

Fig. 1 shows the resulting chromatogram for ten lanthanide elements plus yttrium. The lanthanides are eluted with high yields (80-90 %) in well-separated peaks in a sequence of decreasing ionic radii of the ions in the trivalent state. The resolution is 14 s to 24 s full width at half maximum. The whole gaschromatographic separation can be completed within 430 s. For the separation of the lanthanide group comprising 14 elements a slightly longer time is required with the same resolution of the gaschromatographic peaks.

From the experimental data one can conclude that the separation of trivalent actinide ions should also be possible within a few minutes.

\*and GSI Darmstadt

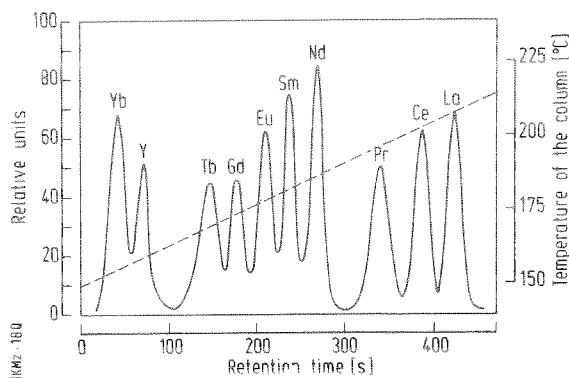


Fig. 1: Temperature-controlled gaschromatographic separation of lanthanide elements in form of  $\text{Ln}(\text{HFA})_3 \cdot 2\text{TOPO}$  complexes. The dashed line represents the temperature time dependence

#### References

- <sup>1</sup>R. Denig, et al., Z. Anal. Chem. 216, 41 (1966)
- <sup>2</sup>W.C. Butts and C.V. Banks, Anal. Chem. 42, 133 (1970)
- <sup>3</sup>N. Greulich et al., GSI Scientific Report 1981, 82-1, 219 (1982)

Separation of Neutron-Rich Neptunium-Isotopes from the Reaction Products of  $^{136}\text{Xe} + ^{244}\text{Pu}$  with the Centrifuge - System SISAK II

H. Tetzlaff, G. Herrmann\*, N. Kaffrell, J.V. Kratz, J. Rogowski, N. Trautmann  
 Institut für Kernchemie, Universität Mainz  
 M. Skalberg, G. Skarnemark  
 Chalmers University of Technology, Göteborg  
 J. Alstad  
 Department of Chemistry, University Oslo  
 M.M. Fowler  
 Los Alamos National Laboratory  
 K.J. Moody, W. Brüche, M. Brügger, H. Gäggeler<sup>†</sup>, M. Schädel, K. Sümmerer  
 GSI Darmstadt

The collision between  $^{136}\text{Xe}$  and  $^{244}\text{Pu}$  is used to produce neutron-rich actinide isotopes. In such reactions, the most probable reaction channels, besides fission, are the transfer of a few nucleons between projectile and target. Thus, neutron-rich isotopes of Pu, Np, U and Pa could be formed. The expected half-lives of the previously unknown neptunium-isotopes 243 and 244 range between a few minutes and a few seconds<sup>1,2</sup>.

For the isolation of the neutron-rich neptunium isotopes a fast separation procedure with the centrifuge system SISAK II was developed as shown in Fig. 1. A target of  $^{244}\text{Pu}$  ( $\approx 1\text{mg/cm}^2$ ) is irradiated with  $^{136}\text{Xe}$  ions at an energy between 750 and 860 MeV. The reaction products recoiling out of the plutonium target are stopped in KCl-cluster loaded argon gas and are transported to the SISAK II-system<sup>3</sup> through a capillary. The transport time is about 10 seconds.

The SISAK II-system consists of three mixer-centrifuge units and a degasser. In the first step of the separation-procedure the KCl-clusters together with the attached reaction products are dissolved in a static mixer in 0.6 M HCl containing 0.3 %  $\text{TiCl}_3$ . With  $\text{TiCl}_3$  neptunium is reduced to the  $3^+$  state. The mixture is pumped to the degassing unit, where the jet-gas and the fission noble gases are separated from the rest of the reaction products. Then the liquid is fed into a mixer-centrifuge unit (1) and contacted with 5 % HDEHP in  $\text{CCl}_4$ . Thorium and uranium together with several fission products are extracted into the organic phase whereas neptunium remains in the aqueous phase. The aqueous phase is mixed with a solution of 6 M  $\text{HNO}_3$ /0.15 M oxalic acid/0.04 M tartaric acid/0.04 M potassiumhydrogentartrate. The nitric acid causes the oxidation of neptunium to the  $4^+$  state. In this form it is extracted into 7 % HDEHP in  $\text{CCl}_4$  in the second mixer-centrifuge unit (2). The complexing agents keep the fission products in the aqueous phase. In the last step the organic phase is pumped into the

third mixer centrifuge unit (3), where neptunium is back-extracted with 15 %  $\text{H}_3\text{PO}_4$ . The chemical yield of the separation procedure is 75 % as was determined with  $^{239}\text{Np}$ . The aqueous phase with the neptunium activity is pumped continuously through a 30 ml measuring cell with a capton window on one side. For X-ray and  $\gamma$ -ray measurements a Ge- and a Ge(Li)-detector were placed in front of the cell.

The  $\gamma$ -ray spectra show, in addition to the  $\gamma$ -lines of the already known  $^{241}\text{Np}$  and  $^{242}\text{Np}$  nuclides, new  $\gamma$ -lines which can be assigned<sup>4</sup> to the yet unknown nuclides  $^{243}\text{Np}$  and  $^{244}\text{Np}$ .

\*and GSI Darmstadt

<sup>†</sup>presently at EIR Würenlingen

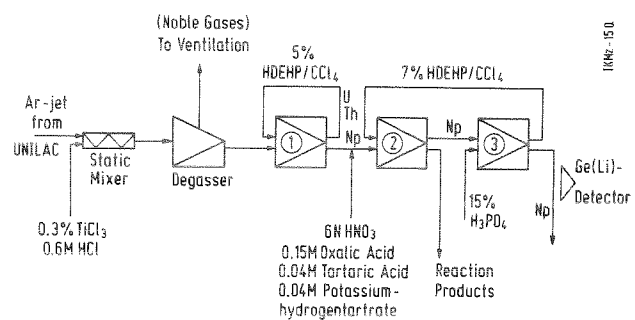


Fig. 1: Separation scheme for the isolation of neptunium from heavy-ion reaction product mixtures  
 (1), (2), (3) = mixer-centrifuge units

#### References

- <sup>1</sup>H.V. Klapdor et al., Atomic Data Nucl. Data Tables 31, 81 (1984)
- <sup>2</sup>K. Takahashi et al., Atomic Data Nucl. Data Tables 12, 101 (1973)
- <sup>3</sup>G. Skarnemark et al., Nucl. Instr. Meth. 171, 323 (1981)
- <sup>4</sup>K.J. Moody et al., this Report

Fast On-Line Chemistry for Zr and Nb<sup>G</sup>

E. Jäger, H. Gäggeler\*, K.J. Moody  
 GSI Darmstadt

N. Greulich, U. Hickmann, N. Trautmann  
 Universität Mainz

In the pioneering fast chemistry experiments from Zvara et al.<sup>1,2</sup> on-line thermochromatography was applied to separate short-lived isotopes of element 104 (Zr or Hf-like) and 105 (Nb or Ta-like) using the formation of volatile chlorides and bromides. In this technique, volatile species are swept by a carrier gas through a tube with a negative temperature gradient and are deposited at certain deposition temperatures. Identification, however, was only possible by fission-track counting on mica detectors inserted into the chromatographic tube. With this respect, a considerable improvement is to use the on-line gaschromatography apparatus<sup>3</sup> (OLGA) connected to a gas-jet transportation system. This technique has already successfully been used to search for short-lived volatile superheavy elements<sup>4</sup>. Here, volatile species are separated in an isothermal tube (SiO<sub>2</sub>) from less volatile compounds and are deposited on a rotating wheel system. From time to time the deposited activity is turned in front of suitable detectors (GeLi, surface-barrier detectors).

In this work, we tried for the first time to use OLGA for separation of short-lived halides. Therefore, at the entrance of the oven system reactive gases such as HCl, HI and HBr were added to the gas-jet (N<sub>2</sub>/KCl) containing the reaction products (fission products from the TRIGA reactor at Mainz University). In the first section of the chromatographic oven (kept at 1000°C) the KCl clusters were destroyed and volatile halides were further transported along an isothermal section kept at variable temperature. Focussing on a fast separation of Zr and Nb (as tracers for elements 104 and 105) it turned out that HBr is better suited than HCl or HI due to technical reasons: With HI the entire apparatus was immediately covered by deposited I<sub>2</sub> and with HCl corrosion problems prevented OLGA to run undisturbed. The volatile bromides were deposited on 100 µm Ni foils mounted onto the wheel and every 3 second the deposited activity was turned by 45° in front of a GeLi detector to measure the fission products by their γ-lines. The following isotopes of Zr and Nb were identified: <sup>99,100,101,102,103,104</sup>Nb, and <sup>99,100,102</sup>Zr, with the shortest-lived nuclide being <sup>103</sup>Nb (T<sub>1/2</sub> = 1,5 sec). In Figs 1 and 2 the deposited activity on the wheel for two typical isotopes (high independent fission yields,

not much feeding by precursors due to β-decay) of Zr and Nb are plotted as function of the isothermal section of the tube. The numbers in parenthesis represent the amount of reactive gas (in Torr) added to the N<sub>2</sub>/KCl-gas-jet.

We observed highest yields for both elements at temperature of about 300 to 400°C. The only difference in the chemical behaviour seems to be the bromide formation affinity: Whereas no significant yield differences for Nb are observed within 10 to 223 Torr HBr, a partial pressure of about 10 Torr in HBr seems to be too low to efficiently form volatile Zr-bromides. This observation will in future be further investigated to develop not only a fast trans-actinide chemistry but also to separate them further into individual elements. Finally, under the conditions shown in Figs 1 and 2 no lanthanide elements were transported along the tube which gives optimism to hope that also heavy actinides (up to Lr) should be well separable from elements ≥ 104.

\* presently at EIR Würenlingen

1. I. Zvara et al., Sov. J. Atomic Energy 21, 709 (1966)
2. I. Zvara et al., Radiokhimiya 18, 371 (1976)
3. K. Sümmerer et al., GSI-84-17 (1984)
4. P. Armbruster et al., LBL-18581 (1984), and submitted to Phys. Rev. Lett.

Figs 1,2: Activities of <sup>100</sup>Zr (Fig. 1) and <sup>104</sup>Nb (Fig. 2), respectively, on the collecting wheel as a function of the oven temperatures.

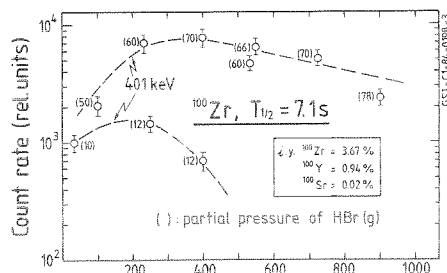


Fig. 1

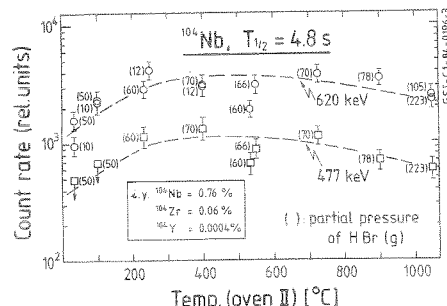


Fig. 2

HIGH Efficiency Heavy Ion Identification System using Low Pressure MWPCs for the Search of Heavy Relic Particles and Stable Strange Matter

M. Brügger, E. Jäger, S. Polikanov (GSI Darmstadt)
A. Breskin, R. Chechik, Z. Fraenkel (Weizmann Institute, Israel)
G. Herrmann, M. Overbeck, N. Trautmann (Univ. Mainz)

A search for heavy relic particles (mass 10 - 10^6 GeV) produced in the early, hot universe and also for the "strange matter" is being pursued via the detection of low energy heavy ions (U) scattered from target samples, which perhaps contain heavy matter, to the backward hemisphere, without significant loss of kinetic energy. A detection system has been designed to register the time of flight, scattering angle and specific ionization of the scattered particles. The reconstructed track information (Target + START and STOP positions) is used to reject events which are scattered from frames, wires and chamber walls. The system is composed of 18 low pressure bidimensional position sensitive and timing detectors covering the backward hemisphere of the target with a solid angle of ~pi Str. Such detectors are particularly suitable for applications in which heavy ions have to be efficiently detected. Six identical START detectors placed in a semicircle at 20 cm distance from the target and 12 identical STOP detectors placed in two rows 60 cm from the target (Fig. 1).

The START detector is an 8x30 cm^2 Multi Wire Proportional Counter (MWPC) of a modular structure. The anodes and cathodes are made of 10um and 50 um wires respectively, 1 mm apart. The anode plane is divided into 4 sections, each of them connected to a fast preamplifier. The signals from the preamplifier are combined with a linear FAN-IN and are further processed by a constant fraction discriminator. Since a rather moderate angular resolution is required in the backscattering experiment, groups of 2 and 3 adjacent wires of the x and y cathode planes, respectively, are connected to the taps of integrated delay-lines. After amplification and shaping, the signals from the delay-lines are used to obtain the position of the avalanche from the time difference between the induced pulses propagating towards the two ends of the delay-line. The time distribution (measured with 120 MeV ^58Ni ions) has a width of 400 ps. The position resolution was found to be ~ 1 mm.

The STOP detector is a 26 x 39 cm^2 MWPC similar to the START detector, but with an additional 20 mm drift space coupled to a Paralleplate Avalanche Counter (PPAC) stage for measurements of specific energy loss. The PPAC planes are made of 50 um wires, 1 mm apart. The anode plane of the STOP detector is divided into 8 sections as described above. On the x and y cathodes

groups of 4 and 5 wires, respectively, are connected to the taps of the delay-lines. The timing and position resolution of the STOP detector is of about the same order as that of the START detector. With a 140 MeV ^100Mo beam a delta E resolution of the order of 10% (FWHM) could be obtained. One module of the full detection system will be tested in the near future with a 1.4 MeV/u ^238U beam.

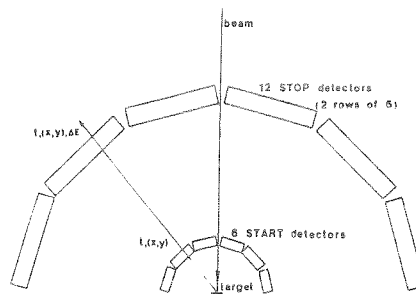


Fig. 1: The detection system

References

a. A. Breskin, R. Chechik, I. Levin, N. Zwang, Nucl. Instr. Meth. 217 (1983) 107